

S²Sent: Nested Selectivity Aware Sentence Representation Learning

Jianxiang Zang¹, Nijia Mo², Yongda Wei², Meiling Ning³, Hui Liu^{2*}

¹ Fudan University, ² Shanghai University of International Business and Economics

³ Beijing University of Posts and Telecommunications,

jxzang25@m.fudan.edu.cn, liuh@suibe.edu.cn

Abstract

The combination of Transformer-based encoders with contrastive learning represents the current mainstream paradigm for sentence representation learning. This paradigm is typically based on the hidden states of the last Transformer block of the encoder. However, within Transformer-based encoders, different blocks exhibit varying degrees of semantic perception ability. From the perspective of interpretability, the semantic perception potential of knowledge neurons is modulated by stimuli, thus rational cross-block representation fusion is a direction worth optimizing. To balance the semantic redundancy and loss across block fusion, we propose a sentence representation selection mechanism S²Sent, which integrates a parameterized nested selector downstream of the Transformer-based encoder. This selector performs spatial selection (SS) and nested frequency selection (FS) from a modular perspective. The SS innovatively employs a spatial squeeze based self-gating mechanism to obtain adaptive weights, which not only achieves fusion with low information redundancy but also captures the dependencies between embedding features. The nested FS replaces GAP with different DCT basis functions to achieve spatial squeeze with low semantic loss. Extensive experiments have demonstrated that S²Sent achieves significant improvements over baseline methods with negligible additional parameters and inference latency, while highlighting high integrability and scalability.

1 Introduction

The integration of Transformer-based encoders and contrastive learning is still the mainstream paradigm for sentence representation learning (Devlin et al., 2019; Liu et al., 2019; Gao et al., 2021; Jiang et al., 2022; Warner et al., 2024). BERT-based embeddings have been successfully

deployed in large-scale retrieval systems (Zhu et al., 2024), achieving high-throughput semantic matching under sub-millisecond latency constraints (Gao et al., 2021). In real-time interactive scenarios, sequence recommendation architectures incorporating sentence representations significantly improve click-through rates through contrastive learning strategies (Zheng et al., 2024; Zang et al., 2025a). For retrieval-augmented generation systems, dynamically distilled sentence embedding optimization substantially reduces computational overhead in real-time semantic matching (Zang and Liu, 2023a,b; Zhao et al., 2024). Enhancing the separation of sentences with distinct semantics through contrastive learning is the main research trend for improving sentence representation learning.

However, an overlooked issue is that these methods typically rely on the hidden states from the last Transformer block of the encoder, with different blocks of the encoder exhibiting varying levels of semantic sensitivity. There is also some work advocates linear fusion of hidden states from different blocks or equal consideration of them during training (Su et al., 2021; Gao et al., 2021; Zhuo et al., 2023). In the field of neuroscience, the semantic potential of neurons is modulated by stimuli, which is not static and is related to the contrast of the stimulus (Nelson and Frost, 1978): the lower the contrast, the stronger the effective semantic perception (Sceniak et al., 1999). From the perspective of interpretability, the lower-level blocks of Transformer-based encoder models encode the basic and structural semantic information (for example, part-of-speech tags), while the later layers encode more “semantic” information (Tenney, 2019). Recently, related studies have found that “knowledge neurons” are distributed in the top several layers of pre-trained encoder models (Dai et al., 2022). Treating the hidden states from different blocks equally is insufficient to model this characteristic and difficult to unleash the semantic perception po-

*Corresponding author.

tential of different blocks. Inspired by this, we propose a novel selectivity aware cross-block fusion mechanism **S²Sent**, which incorporates a parameterized nested selector downstream of Transformer-based encoder. This selector performs a **Spatial Selection (SS)** nested with a **Frequency Selection (FS)**. Through these selections, S²Sent modulates feature extraction at different scales within the encoder, fusing a more potential sentence representation while reducing downstream redundancy and semantic information loss.

The SS module is a selective multi-scale adaptive fusion mechanism that employs a novel spatial squeeze based self-gating mechanism. It employs a squeeze-excitation mechanism to obtain feature representations of hidden states, using them as adaptive weights to fuse the hidden states of each block. This method of determining adaptive weights avoids the information redundancy caused by conflicts between the previous self-gating (Rei and Søgaard, 2019; Stacey et al., 2022) mechanisms and the residual connections in Transformers. It also models dependencies between features that were previously unexplored in Transformers, highlighting features that are crucial for sentence semantics. The FS module, nested within the SS, is a multispectral selective spatial squeeze that leverages the property that the discrete cosine transform (DCT) is an extension of global average pooling (GAP), by selecting low-frequency DCT basis functions for each feature component to be encoded as a scalar. Compared to GAP-based spatial squeeze (Hu et al., 2018; Li et al., 2019, 2023), the FS module largely preserves the expressive power of the feature channels during spatial squeeze.

We evaluate four baseline methods using BERT (Devlin et al., 2019) and RoBERTa (Liu et al., 2019) as backbones, and perform unsupervised sentence embedding training with SimCSE (Gao et al., 2021) and PromptCSE (Jiang et al., 2022). We analyze the impact of S²Sent on these baselines across seven STS tasks. Extensive experimental results demonstrate that S²Sent is compatible with all Transformer-based encoders and can significantly enhance the sentence representation capability of the backbone with only negligible increases in additional parameters and inference latency. The ablation studies further emphasize the contributions of these two selection mechanisms. Through the discussion of hyperparameters, we were pleasantly surprised to find that S²Sent does not rely on the selection of hyperparameters such

as the number of Transformer blocks or the frequency components, demonstrating strong integrability and scalability. Our primary contributions are highlighted as follows:

- We propose a novel sentence representation mechanism, S²Sent. S²Sent achieves efficient sentence representation fusion across Transformer blocks by leveraging Spatial Selection (SS) and nested Frequency Selection (FS).
- SS introduces a novel self-gating mechanism that assigns spatially squeezed feature representations as adaptive weights to achieve representation fusion. This method not only reduces information redundancy but also models the dependencies between embedding features.
- FS selects different low-frequency DCT basis functions to weight and squeeze feature parts, thereby reducing the loss associated with feature channel scalarization.
- S²Sent is compatible with all Transformer-based encoders, and the additional parameters and inference latency it introduces are negligible compared to the backbone network. Moreover, the optimization it brings does not rely on the choice of hyperparameters, demonstrating its high integrability and scalability.

2 Related Work

2.1 Sentence Representation Learning

Amidst the recent surge in large language models, the task of sentence representation based on LLMs continues to struggle to achieve satisfactory performance. These models are predominantly trained on text continuation tasks, where the loss function primarily focuses on the accuracy of predicting the next token, rather than evaluating the quality of the overall sentence representation (Zhu et al., 2023; Wang et al., 2024). Accordingly, Transformer-based pre-trained encoders are still the mainstream sentence representation backbone, adopting an end-to-end approach (Devlin et al., 2019; Liu et al., 2019; He et al., 2020). However, these methods encode sentences out-of-the-box, leading to issues such as anisotropy in the representation space (Ethayarajh, 2019; Zhang et al., 2020; Zang et al., 2025b). Some efforts have been made to transform the representation space into a smooth

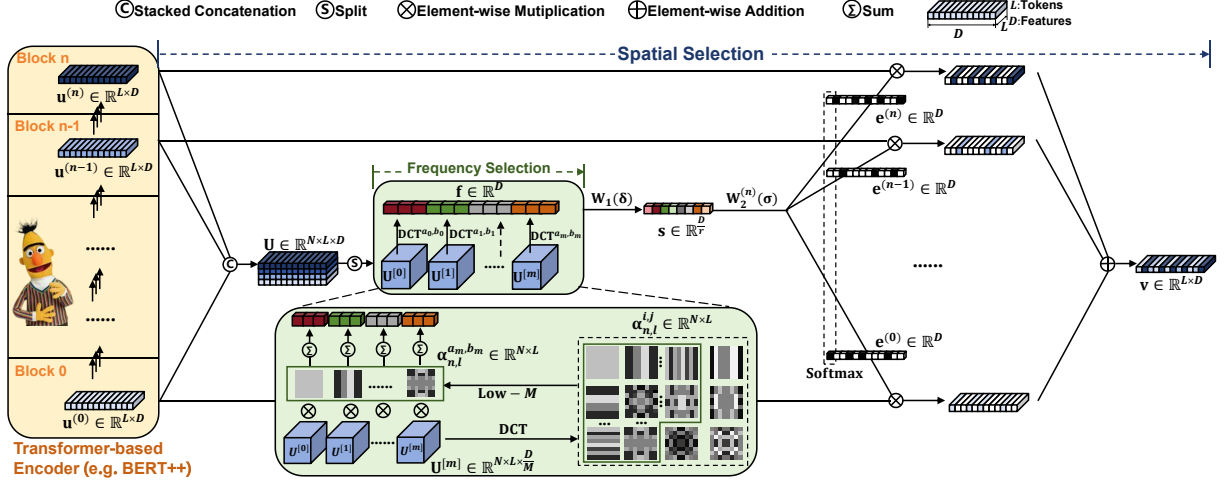


Figure 1: Overview of S^2 Sent. S^2 Sent builds a parameterized nested selector downstream of Transformer-based encoder, which performs a Spatial Selection (SS) nested with Frequency Selection (FS).

and isotropic space (Li et al., 2020; Su et al., 2021; Zhuo et al., 2023). Contrastive learning methods, on the other hand, aim to tightly combine semantically similar examples while further separating different examples (Gao et al., 2021; Zhang et al., 2022; Jiang et al., 2022), and have emerged as mainstream learning approaches. However, a neglected perspective is that these methods are based on the hidden states from the last Transformer block of the encoder. There is also some work that considers the linear fusion of hidden states from different blocks or equal consideration of them during training (Su et al., 2021; Gao et al., 2021; Zhuo et al., 2023).

However, treating them equally cannot model the adaptive semantic perception of different blocks, and we will demonstrate this in the discussion of the motivation for S^2 Sent.

2.2 Self-Gate for Composing Sentence Representation

The difficulty of learning to construct sentence representations in end-to-end systems lies in the fact that natural language is highly compositional. Related studies have (Rei and Søgaard, 2019; Zang and Liu, 2024a) proposed a self-gate based sentence representation learning architecture. This architecture first activates relevance scores for each token, which can be seen as adaptive weights. The attention weights are then fused with the token sequence embeddings to form the final sentence representation. This self-gate mechanism essentially functions as a sequence tagging system, guiding the encoder to identify important domains in the sentence. Related work has applied this (Stacey et al.,

2022) to downstream Transformer-based encoders. However, these methods activate token representations and fusion mechanisms that are essentially consistent with the feed-forward neural networks and residual connections in the Transformer, leading to information redundancy.

In contrast, we advocate for spatial squeeze to obtain sentence feature representations as adaptive weights for the self-gating mechanism in SS module. This not only achieves low-redundancy fusion but also models feature dependencies that were not present in the Transformer.

2.3 Spatial Squeeze for Feature Representation

Channel attention mechanisms have demonstrated exceptional performance in computer vision tasks (Hu et al., 2018; Woo et al., 2018; Hou et al., 2020). The squeeze-and-excitation network (SE-Net) (Hu et al., 2018) pioneered channel attention by effectively capturing interdependencies among channels through spatial squeeze of feature maps. Subsequent studies, such as CBAM (Woo et al., 2018), SK (Li et al., 2019), LSK (Li et al., 2023), SFA (Zang and Liu, 2024b), DDualSE (Mo et al., 2025), expanded on this idea by incorporating various spatial encoding or attention mechanisms. Inspired by these developments, we propose to leverage downstream attention to model dependencies among semantic embedding features and enhance semantic representation. However, the core spatial squeeze techniques in these approaches still rely on GAP and simply averaging the feature channels for scalarization inevitably leads to significant

Symbol	Interpretation	Symbol	Interpretation
\mathbf{W}	Trainable parameters	$\cdot_{n,l}$	Spatial Descriptor
N	Transformer blocks number	\cdot_d	Feature Descriptor
L	Sentence Length	$<; >$	Dimensional Concatenation
D	Embedding dimension	$[:]$	Stacked Concatenation
δ	Tanh Fuction	σ	Sigmoid Fuction

Table 1: Symbol description sheet

semantic loss.

In contrast, we consider adopting the DCT extension of GAP, utilizing more high-frequency components to achieve spatial squeeze in FS module.

3 Methodology

In this work, we propose a novel sentence representation method, S²Sent. It is essentially a nested selectivity aware representation fusion mechanism across Transformer blocks, where this sophisticated nested selection mechanism minimizes semantic redundancy and loss to the greatest extent possible. As illustrated in Figure 1, S²Sent builds a downstream parameterized selector based on the Transformer-based encoder, performing a tensor mapping: $\{\mathbf{u}^{(n)}\}_{n=0}^{N-1} \rightarrow \mathbf{v}$. Here, $\mathbf{u}^{(n)} \in \mathbb{R}^{L \times D}$ denotes the hidden states from each Transformer block, and $\mathbf{v} \in \mathbb{R}^{L \times D}$ denotes the final sentence representation after optimization by the selector. From a modular perspective, S²Sent performs a Spatial Selection nested with Frequency Selection. The symbols in this paper are explained in Table 1.

3.1 Spatial Selection

3.1.1 Spatial Squeeze based Self-Gate for Adaptive Weights

The key to achieving cross-block sentence representation fusion lies in the calculation of adaptive weights, and the self-gate mechanism is the standard means to achieve adaptivity. Traditional self-gate methods obtain token-level activations as adaptive weights to guide the encoder to focus on important tokens in the sentence, as shown in Figure 2. However, these methods' activation of token representations and fusion mechanisms are essentially consistent with the feed-forward neural network and residual connection in Transformer, which undoubtedly leads to redundant information.

Therefore, we advocate adopting the squeeze-excitation concept, which compresses the representation space to the feature-level representation and models dependencies at the feature level. As shown in Figure 3, using the activated compressed feature representation as adaptive weights can guide

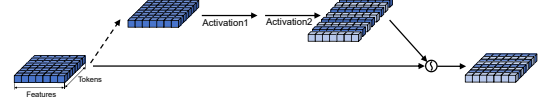


Figure 2: Traditional self-gate mechanism (consistent with the residual connection in Transformer).



Figure 3: spatial squeeze self-gate mechanism.

the focus on features meaningful to sentence representation, an angle of modeling not covered by Transformer. Undoubtedly, this low-information-redundancy self-gate mechanism is the first choice as adaptive fusion weights for sentence representation.

3.1.2 SS Module

Spatial Selection is a selective multiscale adaptive fusion mechanism with the input $\{\mathbf{u}^{(n)}\}_{n=0}^{N-1}$ and output \mathbf{v} . It consists of three stages: concatenation, squeeze-and-excitation, and selection. To capture the nonlinear transformations at the block-token level during the concatenation stage, we propose stacking the sentence representations of each block to build a 3D semantic space $\mathbf{U} \in \mathbb{R}^{N \times L \times D}$, as formulated in Equation 1.

$$\mathbf{U}_{n,l} = [\mathbf{u}_l^{(0)}; \dots; \mathbf{u}_l^{(n)}] \quad (1)$$

In the subsequent squeeze-and-excitation stage, we utilize Frequency Selection to perform spatial squeeze, as formulated in Equation 2. Here, $\mathbf{f} \in \mathbb{R}^D$ denotes the squeezed feature representation, and we will discuss the specific methods of FS in detail in Section 3.2.

$$\mathbf{f}_d = \text{FS}(\mathbf{U}_{n,l,d}) \quad (2)$$

To capture the excited features and adaptively adjust their importance in the overall semantics, we employ a dimensional-reduction fully connected layer (\mathbf{W}_1) and dimensional-augmentation fully connected layers ($\mathbf{W}_2^{(n)}$) with the same number of Transformer blocks in the excitation stage. This allows us to obtain the excited vectors $\{\mathbf{e}^{(n)}\}_{n=0}^{N-1}$, where $\mathbf{e}^{(n)} \in \mathbb{R}^D$, as formulated in Equation 3. The surplus vector $\mathbf{s} = \max(0, \mathbf{f}\mathbf{W}_1) \in \mathbb{R}^{\frac{D}{r}}$ forms a low-rank bottleneck. Here, δ , σ represent the Tanh, Sigmoid functions respectively, and r acts as a reduction ratio that creates a bottleneck structure for parameter redundancy reduction.

$$\mathbf{e}_d^{(n)} = \frac{1}{1 + \exp(-\max(0, \mathbf{f}_d \mathbf{W}_1) \mathbf{W}_2^{(n)})} \quad (3)$$

In the selection stage, we perform softmax normalization on the excitation vectors $\{\mathbf{e}^{(n)}\}_{n=0}^{N-1}$. The normalized results serve as weights for different branches. These weights are element-wise multiplied with the corresponding hidden states $\{\mathbf{u}^{(n)}\}_{n=0}^{N-1}$ and summed to obtain \mathbf{v}_d as the final sentence representation.

$$\mathbf{v}_d = \frac{\sum_{n=0}^{N-1} \exp(\mathbf{e}_d^{(n)}) * \mathbf{u}_d^{(n)}}{\sum_{n=0}^{N-1} \exp(\mathbf{e}_d^{(n)})} \quad (4)$$

3.2 Frequency Selection

3.2.1 DCT: Extension of GAP for Spatial Squeeze

The above mentioned FS module nested within SS performs spatial squeeze to obtain feature representations, where $\mathbf{U} \in \mathbb{R}^{N \times L \times D}$ and $\mathbf{f} \in \mathbb{R}^D$. Inspired by channel attention, a classic approach is to use GAP to average the features across the N and L dimensions. However, this approach undoubtedly reduces the feature differences at different spatial levels, leading to inevitable semantic loss. We will demonstrate in this section that DCT is a better choice for spatial squeeze compared to GAP.

DCT is a widely used data compression method in signal processing, particularly for digital images and videos. First, let us review the general form of a DCT as formulated in Equation 5. Here, α represents the corresponding DCT frequency basis functions. It is worth noting that, for the sake of simplicity, the normalization constant factor of DCT has been omitted.

$$\begin{aligned} \text{DCT}(\mathbf{X}_{i,j}) &= \sum_{i=0}^{N-1} \sum_{j=0}^{L-1} \mathbf{X}_{i,j} \alpha_{n,l}^{i,j}, \\ \alpha_{n,l}^{i,j} &= \cos\left(\frac{\pi n}{N}\left(i + \frac{1}{2}\right)\right) \cos\left(\frac{\pi l}{L}\left(j + \frac{1}{2}\right)\right) \\ \text{Inverse Transform: } \mathbf{X}_{i,j} &= \text{IDCT} \sum_{n=0}^{N-1} \sum_{l=0}^{L-1} \mathbf{x}_{n,l} \alpha_{n,l}^{i,j} \end{aligned} \quad (5)$$

To relate GAP to DCT, we extend the representation of GAP as formulated in Equation 6.

$$\begin{aligned} \text{GAP}(\mathbf{X}_{i,j}) &= \frac{1}{NL} \sum_{i=0}^{N-1} \sum_{j=0}^{L-1} \mathbf{X}_{i,j} \\ &= \frac{1}{NL} \sum_{i=0}^{N-1} \sum_{j=0}^{L-1} \mathbf{X}_{i,j} \cos\left(\frac{\pi * 0}{N}\left(i + \frac{1}{2}\right)\right) \cos\left(\frac{\pi * 0}{L}\left(j + \frac{1}{2}\right)\right) \\ &= \frac{1}{NL} \sum_{i=0}^{N-1} \sum_{j=0}^{L-1} \mathbf{X}_{i,j} \alpha_{0,0}^{i,j} = \frac{1}{NL} \mathbf{x}_{0,0} \end{aligned} \quad (6)$$

$\mathbf{x}_{0,0}$ represents the lowest frequency component of DCT and is directly proportional to GAP. After establishing this point, we can rewrite the inverse transformation of DCT as formulated in Equation 7, which naturally decomposes the semantic spatial information into a combination of different frequency components.

$$\begin{aligned} \mathbf{X}_{i,j} &= \sum_{n=0}^{N-1} \sum_{l=0}^{L-1} \mathbf{x}_{n,l} \alpha_{n,l}^{i,j} \\ &= \mathbf{x}_{0,0} \alpha_{0,0}^{i,j} + \mathbf{x}_{0,1} \alpha_{0,1}^{i,j} + \dots + \mathbf{x}_{N-1,L-1} \alpha_{N-1,L-1}^{i,j} \\ &= NL \text{GAP}(\mathbf{X}_{i,j}) \alpha_{0,0}^{i,j} + \dots + \mathbf{x}_{N-1,L-1} \alpha_{N-1,L-1}^{i,j} \end{aligned} \quad (7)$$

From the perspective of feature descriptor, Equation 8 shows that the representation of each feature under the GAP operation only utilizes the lowest frequency component (✓) of the DCT, while discarding additional higher frequency components (✗). This implies that compared to GAP, DCT can explore a broader range of high-frequency components.

$$\begin{aligned} \mathbf{X}_{i,j} &= \begin{bmatrix} \underbrace{\mathcal{P} \alpha_{0,0}^{0,0}}_{\checkmark} + \underbrace{\mathcal{D}^{0,0}}_{\times} & \dots & \underbrace{\mathcal{P} \alpha_{0,0}^{0,L-1}}_{\checkmark} + \underbrace{\mathcal{D}^{0,L-1}}_{\times} \\ \vdots & \ddots & \vdots \\ \underbrace{\mathcal{P} \alpha_{0,0}^{N-1,0}}_{\checkmark} + \underbrace{\mathcal{D}^{N-1,0}}_{\times} & \dots & \underbrace{\mathcal{P} \alpha_{0,0}^{N-1,L-1}}_{\checkmark} + \underbrace{\mathcal{D}^{N-1,L-1}}_{\times} \end{bmatrix}, \\ \mathcal{P} &= NL \text{GAP}(\mathbf{X}_{i,j}), \\ \mathcal{D}^{i,j} &= \mathbf{x}_{0,1} \alpha_{0,1}^{i,j} + \dots + \mathbf{x}_{N-1,L-1} \alpha_{N-1,L-1}^{i,j} \end{aligned} \quad (8)$$

3.2.2 FS Module

Frequency Selection is a multi-spectral with the input \mathbf{U} and the output \mathbf{f} . It selects appropriate DCT frequency basis functions for each feature. For the input \mathbf{U} , we first split it into m parts along the feature dimension, as formulated in Equation 9. Here, $\mathbf{U}_{n,l}^{[m]} \in \mathbb{R}^{N \times L \times \frac{D}{M}}$.

$$\mathbf{U}_{n,l} \xrightarrow{\text{Split}} \langle \mathbf{U}_{n,l}^{[0]}; \dots; \mathbf{U}_{n,l}^{[m]} \rangle \quad (9)$$

For each part $\mathbf{U}^{[m]}$, we perform spatial squeeze using selected 2D DCT basis functions, as formu-

Low —→ High					
Low —→ High	Low-1	Low-2	Low-8	Low-16	Low-16
	Low-4	Low-4	Low-8	Low-16	Low-16
	Low-8	Low-8	Low-16		
	Low-16	Low-16			
	Low-16				

Figure 4: Selection for m low frequency basis functions

lated in Equation 10, where a_m and b_m are the two-dimensional indices of the frequency basis functions corresponding to $\mathbf{U}^{[m]}$. Previous studies (Hu et al., 2018; Xu et al., 2020) have shown that neural networks tend to be biased towards low-frequency information. Therefore, in the FS module, we select the lowest m frequency basis functions. In the experimental section, we explore different values of m from $\{1 \text{ (GAP)}, 2, 4, 8, 16\}$. The specific selection mechanism is illustrated in Figure 4. Here, $\mathbf{f}^{[m]} \in \mathbb{R}^{\frac{D}{M}}$ denotes the squeezed feature representation of m^{th} part.

$$\begin{aligned} \mathbf{f}_{d'}^{[m]} &= \text{DCT}^{a_m, b_m}(\mathbf{U}^{[m]}) \\ &= \sum_{n=0}^{N-1} \sum_{l=0}^{L-1} \mathbf{U}_{n,l,d'}^{[m]} \alpha_{n,l}^{a_m, b_m} \end{aligned} \quad (10)$$

Finally, we concatenate the m part feature representations $\mathbf{f}_{d'}^{[m]}$ along the dimensions to obtain the final squeezed feature representation, as formulated in Equation 11.

$$\mathbf{f}_d = \langle \mathbf{f}_{d'}^{[0]}; \dots; \mathbf{f}_{d'}^{[m]} \rangle \quad (11)$$

4 Experimental Setup

4.1 Implementation

We used BERT (Devlin et al., 2019) and RoBERTa (Liu et al., 2019) as the backbone models. For training sentence embeddings, we employed two unsupervised contrastive learning methods: SimCSE (Gao et al., 2021) and PromptCSE (Jiang et al., 2022). We represented sentences as the average of all token embeddings. During training, the learning rate was set to 3×10^{-5} for SimCSE and 1×10^{-5} for PromptCSE. We used a batch size of 64 and set the training temperature τ to 0.05. For BERT, we used 384 groups, while for RoBERTa, we used 256 groups. The positive number was set to 3 for all models. The model was evaluated every 125 steps on the

STS-B dev set, and the best checkpoint was used for testing. Experiments were conducted on seven V100 GPUs.

4.2 Benchmarks

We evaluated our method on the Semantic Textual Similarity (STS) task using SentEval (Conneau and Kiela, 2018), which provides a comprehensive evaluation framework for multiple tasks. The STS tasks consists of: STS 2012-2016 (Agirre et al., 2012, 2013, 2014, 2015, 2016), STS Benchmark (Cer et al., 2017), and SICK Relatedness (Marelli et al., 2014).

5 Experimental Results

5.1 Main Results

In this section, we utilized two backbones, BERT and RoBERTa, along with two sentence embedding training methods, SimCSE and PromptCSE, to establish four baseline models. By controlling variables, we examined the impact of the two selections of S^2Sent , SS and FS, on these baseline models for sentence representation.

5.1.1 Effect of Spatial Selection

We first controlled the FS module and explored the impact of SS on the four baseline models. Table 2 reports the Spearman correlation coefficients for STS-Benchmark, SICK-Relatedness, and the average across seven benchmarks, while also presenting the additional parameters and inference latency introduced. A higher Spearman correlation coefficient indicates a stronger positive correlation between the two statistical variables. In each set of experiments, **Base** refers to our recalculated baseline results using only the Last1 block for representation. Table 2 also presents the effects of using different block representations (Last1, Last3, Last6) and various downstream sentence representation strategies on the baseline results. Our experimental results are averaged over 7 random seeds. The **value** indicates a significant improvement over the base (based on t-tests), and the **value** represents the best result in the group.

It is evident that for the Last3 and Last6 strategies, simply averaging the representations does not significantly improve over the base set using Last1. However, introducing S^2Sent (1D SS) for representation optimization after averaging leads to significant improvements across all experimental sets, demonstrating the effectiveness of SS in

Backbone	Block	Downstream	Δ Param.	Δ Latency	SimCSE			PromptCSE		
					STS-B	SICK-R	STS-Avg.	STS-B	SICK-R	STS-Avg.
BERT	Last1	-Base	-	-	76.88	72.19	76.21	81.70	69.57	78.11
		-S ² Sent(1D SS)	0.08%	0.20%	77.82	71.98	77.18	82.34	69.78	79.85
		-Avg.	0.00%	0.00%	77.25	72.05	76.48	82.06	69.89	79.22
	Last3	-Avg.-S ² Sent(1D SS)	0.08%	0.20%	77.79	72.05	77.02	82.62	69.62	79.71
		-Stack-S ² Sent(2D SS)	0.17%	0.20%	79.54	73.18	78.50	83.41	71.15	80.98
		-Avg.	0.00%	0.00%	76.73	72.21	76.17	81.81	69.92	79.50
	Last6	-Avg.-S ² Sent(1D SS)	0.08%	0.20%	77.87	71.75	77.06	82.19	69.82	79.90
		-Stack-S ² Sent(2D SS)	0.34%	0.20%	79.23	73.03	78.14	83.58	70.97	80.81
RoBERTa	Last1	-Base	-	-	80.32	68.51	76.46	81.81	69.74	79.02
		-S ² Sent(1D SS)	0.07%	0.19%	81.68	69.25	78.19	82.17	70.34	79.80
		-Avg.	0.00%	0.00%	80.73	68.47	76.61	81.97	69.89	79.61
	Last3	-Avg.-S ² Sent(1D SS)	0.07%	0.19%	81.97	69.11	78.35	81.98	69.82	80.36
		-Stack-S ² Sent(2D SS)	0.15%	0.19%	82.57	70.95	78.32	83.91	71.21	81.18
		-Avg.	0.00%	0.00%	80.13	68.60	76.53	81.77	69.98	79.50
	Last6	-Avg.-S ² Sent(1D SS)	0.07%	0.19%	81.81	69.23	78.26	82.08	70.34	79.98
		-Stack-S ² Sent(2D SS)	0.30%	0.19%	82.41	70.89	78.48	83.67	71.57	81.25

Table 2: Study for SS, evaluation results on STS tasks

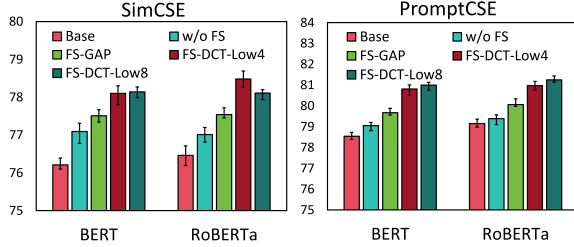


Figure 5: Study for FS, evaluation results on STS tasks

S²Sent. Furthermore, the standard implementation of S²Sent(2D SS), which stacks and concatenates representations from different blocks, achieves the best results in all groups. This indicates that using 3D tensors for downstream modeling with stacked and concatenated representations better preserves the hierarchical semantic information across different Transformer blocks. Based on the reported additional overhead of S²Sent, we can observe that the introduced parameters amount to less than 0.5% of the backbone, which is superior to the bottleneck layer set in SS. Similarly, the inference latency introduced is extremely low, as it does not involve high-cost attention mechanisms like cross-attention, and the inference of multiple branches can be processed in parallel. Overall, S²Sent is undoubtedly a lightweight module.

5.1.2 Effect of Frequency Selection

Additionally, we controlled all conditions in SS to be optimally set, and in this section, we discuss the role of FS. Figure 5 illustrates the impact of the following cases: (1) no FS for spatial squeeze, (2) using GAP for squeeze, (3) using Low-4 DCT

basis functions, and (4) using Low-8 DCT basis functions for squeeze. Figure 5 shows the averages across the seven STS tasks for each case.

When FS was not used for spatial squeezing and activation was directly performed using fully connected layers, S²Sent showed some improvement in the sentence representation capability of the backbone. This indicates the effectiveness of the multi-scale adaptive fusion mechanism. Introducing FS for spatial squeeze further enhanced the backbone’s representation capability. This is because the feature representation, activated by the spatially squeezed features, models the dependencies between different embedding features. DCT-based spatial squeezing outperforms GAP. Using 4 and 8 low-frequency basis functions achieved the best performance across combinations of two backbone models and two contrastive learning methods. This demonstrates that DCT offers better potential for spatial squeeze as an extension of GAP.

5.2 Hyperparameter

5.2.1 Effect of m & n

Table 2 and Figure 5 offer preliminary insights into cases where m is Last3 and Last6, and n is Low4 and Low8. In this section, we conducted more comprehensive experiments for in-depth analysis. Figure 6 illustrates the impact of the selected number of Transformer blocks (n) and the chosen number of low-frequency DCT basis functions (m) on the performance of four baselines. For the hyperparameter n , we conducted five sets of experiments using representations from the last1, 3, 6, 9, and

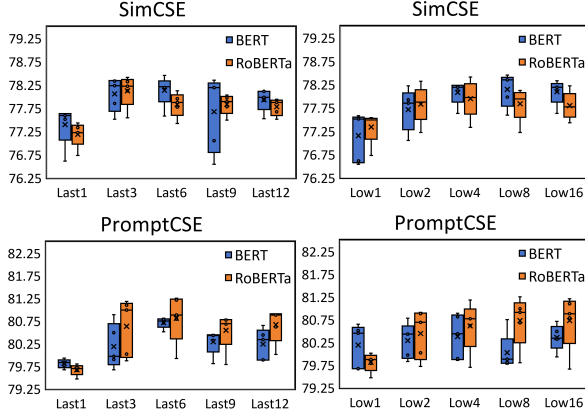


Figure 6: The impact of n (left) and m (right).

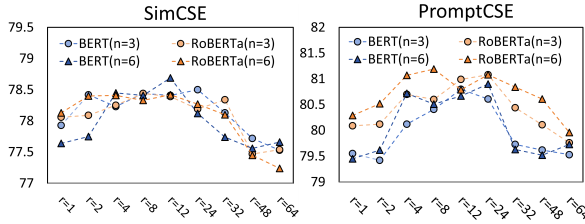


Figure 7: The impact of r

12 Transformer blocks, respectively. For each set, we selected m from low1, 2, 4, 8, and 16 to obtain five data points, which were then plotted as box plots. The same procedure was applied to the hyperparameter m .

Figure 6 shows that when n was set to last1 and m was set to low1, which corresponds to using the last hidden state of the Transformer as the representation and applying GAP for spatial squeeze—the model performs the worst across all cases. However, when m and n were set to values greater than 1, the model’s performance significantly improved with minimal variation between them. This means that in practice, we only need to select blocks and frequency components greater than 1. This result is encouraging as it highlights the effectiveness of our approach while reducing the dependence on hyperparameter tuning, thereby demonstrating the ease of integration of S^2 Sent.

5.2.2 Effect of Reduction ratio r

The reduction ratio r constructs a bottleneck layer in the excitation stage. Its size is linearly negatively correlated with the model size to reduce parameter redundancy. We conducted experiments with various values of r , and the comparison shown in Figure 7 indicates that the performance of the baseline initially increases and then decreases as r increases. This is likely because a very small r

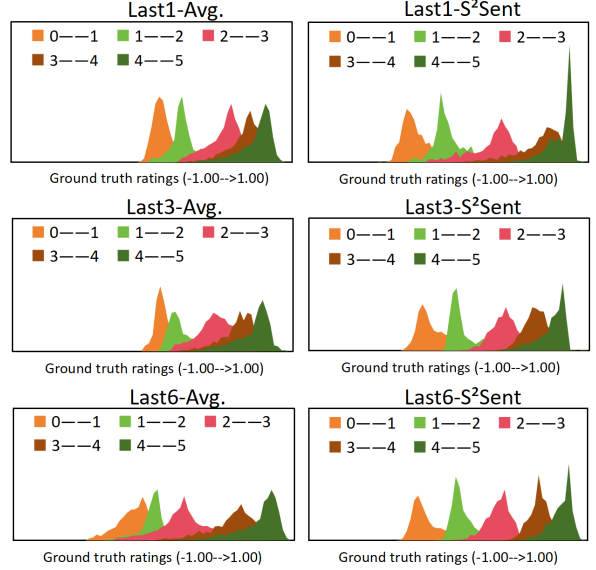


Figure 8: Density plots of cosine similarities between sentence pairs in STS-B. Pairs are divided into 5 groups based on ground truth ratings (higher means more similar) along the y-axis, and x-axis is the cosine similarity.

results in a large number of parameters, leading to overfitting. Conversely, an excessively large r can impair the module’s expressive power due to an overly reduced bottleneck. Therefore, values of r ranging from 4 to 24 are all considered feasible.

5.3 Case Study

To directly demonstrate the advantages of our method on the STS task, we present in Figure 8 the cosine similarity distributions of STS-B sentence pairs using BERT-SimCSE and their corresponding human ratings. Specifically, we compare the direct fusion of hidden states from different blocks (last 1, 3, 6) as sentence representations in the baseline approach with the utilization of S^2 Sent for optimizing sentence representations. Compared to the direct fusion of hidden states from different blocks, the baselines incorporating S^2 Sent exhibit a more scattered distribution of cosine similarities while maintaining lower variance, even for semantically similar sentence pairs. This indicates that S^2 Sent provides better differentiation of sentence pairs with varying degrees of similarity.

6 Conclusion

We propose an innovative sentence representation technique called S^2 Sent, which builds a parameterized nested selector downstream of a Transformer-based encoder for cross block representation fusion. The nested selector consists of Spatial Selection

(SS) and Frequency Selection (FS) nested within SS. SS is a selective multi-scale adaptive fusion technique, while FS is a multi-spectral selective spatial squeeze. S²Sent enables effective sentence representation fusion across different blocks while minimizing the loss or redundancy of semantic information in downstream tasks. Beyond sentence representation, the framework of S²Sent is applicable to stack-based or Inception-based encoding structures, revealing its potential in other application scenarios.

7 Limitations

Considering the differences in sentence representation training paradigms, our S²Sent is suitable for transformer-based encoder pre-trained models but not applicable to training sentence embeddings with generative LLMs. Whether generative LLM-based sentence representations can support such dynamic cross-layer representation fusion remains an open question worth exploring.

References

- Eneko Agirre, Carmen Banea, Claire Cardie, Daniel Cer, Mona Diab, Aitor Gonzalez-Agirre, Weiwei Guo, Inigo Lopez-Gazpio, Montse Maritxalar, Rada Mihalcea, et al. 2015. Semeval-2015 task 2: Semantic textual similarity, english, spanish and pilot on interpretability. In *Proceedings of the 9th international workshop on semantic evaluation (SemEval 2015)*, pages 252–263.
- Eneko Agirre, Carmen Banea, Claire Cardie, Daniel Cer, Mona Diab, Aitor Gonzalez-Agirre, Weiwei Guo, Rada Mihalcea, German Rigau, and Janyce Wiebe. 2014. Semeval-2014 task 10: Multilingual semantic textual similarity. In *Proceedings of the 8th international workshop on semantic evaluation (SemEval 2014)*, pages 81–91.
- Eneko Agirre, Carmen Banea, Daniel Cer, Mona Diab, Aitor Gonzalez Agirre, Rada Mihalcea, German Rigau Claramunt, and Janyce Wiebe. 2016. Semeval-2016 task 1: Semantic textual similarity, monolingual and cross-lingual evaluation. In *SemEval-2016. 10th International Workshop on Semantic Evaluation; 2016 Jun 16-17; San Diego, CA. Stroudsburg (PA): ACL; 2016. p. 497-511. ACL (Association for Computational Linguistics)*.
- Eneko Agirre, Daniel Cer, Mona Diab, and Aitor Gonzalez-Agirre. 2012. Semeval-2012 task 6: A pilot on semantic textual similarity.* sem 2012: The first joint conference on lexical and computational semantics—. In *Proceedings of the Sixth International Workshop on Semantic Evaluation (SemEval 2012)*, Montréal, QC, Canada, pages 7–8.
- Eneko Agirre, Daniel Cer, Mona Diab, Aitor Gonzalez-Agirre, and Weiwei Guo. 2013. * sem 2013 shared task: Semantic textual similarity. In *Second joint conference on lexical and computational semantics (*SEM), volume 1: proceedings of the Main conference and the shared task: semantic textual similarity*, pages 32–43.
- Daniel Cer, Mona Diab, Eneko Agirre, Iñigo Lopez-Gazpio, and Lucia Specia. 2017. Semeval-2017 task 1: Semantic textual similarity multilingual and crosslingual focused evaluation. In *Proceedings of the 11th International Workshop on Semantic Evaluation (SemEval-2017)*, pages 1–14.
- Alexis Conneau and Douwe Kiela. 2018. Senteval: An evaluation toolkit for universal sentence representations. In *Proceedings of the Eleventh International Conference on Language Resources and Evaluation (LREC 2018)*.
- Damai Dai, Li Dong, Yaru Hao, Zhifang Sui, Baobao Chang, and Furu Wei. 2022. Knowledge neurons in pretrained transformers. In *Proceedings of the 60th Annual Meeting of the Association for Computational Linguistics (Volume 1: Long Papers)*, pages 8493–8502.
- Jacob Devlin, Ming-Wei Chang, Kenton Lee, and Kristina Toutanova. 2019. Bert: Pre-training of deep bidirectional transformers for language understanding. In *Proceedings of the 2019 Conference of the North American Chapter of the Association for Computational Linguistics: Human Language Technologies, Volume 1 (Long and Short Papers)*, pages 4171–4186.
- Kawin Ethayarajh. 2019. How contextual are contextualized word representations? comparing the geometry of bert, elmo, and gpt-2 embeddings. In *Proceedings of the 2019 Conference on Empirical Methods in Natural Language Processing and the 9th International Joint Conference on Natural Language Processing (EMNLP-IJCNLP)*, pages 55–65.
- Tianyu Gao, Xingcheng Yao, and Danqi Chen. 2021. Simcse: Simple contrastive learning of sentence embeddings. In *Proceedings of the 2021 Conference on Empirical Methods in Natural Language Processing*, pages 6894–6910.
- Pengcheng He, Xiaodong Liu, Jianfeng Gao, and Weizhu Chen. 2020. Deberta: Decoding-enhanced bert with disentangled attention. *arXiv preprint arXiv:2006.03654*.
- Qibin Hou, Li Zhang, Ming-Ming Cheng, and Jiashi Feng. 2020. Strip pooling: Rethinking spatial pooling for scene parsing. In *Proceedings of the IEEE/CVF conference on computer vision and pattern recognition*, pages 4003–4012.
- Jie Hu, Li Shen, and Gang Sun. 2018. Squeeze-and-excitation networks. In *Proceedings of the IEEE conference on Computer Vision and Pattern Recognition*, pages 7132–7141.

- Ting Jiang, Jian Jiao, Shaohan Huang, Zihan Zhang, Deqing Wang, Fuzhen Zhuang, Furu Wei, Haizhen Huang, Denvy Deng, and Qi Zhang. 2022. Promptbert: Improving bert sentence embeddings with prompts. In *Proceedings of the 2022 Conference on Empirical Methods in Natural Language Processing*, pages 8826–8837.
- Bohan Li, Hao Zhou, Junxian He, Mingxuan Wang, Yiming Yang, and Lei Li. 2020. On the sentence embeddings from pre-trained language models. In *Proceedings of the 2020 Conference on Empirical Methods in Natural Language Processing (EMNLP)*, pages 9119–9130.
- Xiang Li, Wenhai Wang, Xiaolin Hu, and Jian Yang. 2019. Selective kernel networks. In *Proceedings of the IEEE/CVF conference on computer vision and pattern recognition*, pages 510–519.
- Yuxuan Li, Qibin Hou, Zhaohui Zheng, Ming-Ming Cheng, Jian Yang, and Xiang Li. 2023. Large selective kernel network for remote sensing object detection. In *Proceedings of the IEEE/CVF International Conference on Computer Vision*, pages 16794–16805.
- Yinhan Liu, Myle Ott, Naman Goyal, Jingfei Du, Mandar Joshi, Danqi Chen, Omer Levy, Mike Lewis, Luke Zettlemoyer, and Veselin Stoyanov. 2019. Roberta: A robustly optimized bert pretraining approach. *arXiv preprint arXiv:1907.11692*.
- Marco Marelli, Luisa Bentivogli, Marco Baroni, Raffaella Bernardi, Stefano Menini, and Roberto Zamparelli. 2014. Semeval-2014 task 1: Evaluation of compositional distributional semantic models on full sentences through semantic relatedness and textual entailment. In *Proceedings of the 8th international workshop on semantic evaluation (SemEval 2014)*, pages 1–8.
- Nijia Mo, Jianxiang Zang, Zhan Wang, and Hui Liu. 2025. Ddualse: Decoupled dual-head squeeze and excitation attention for sequential recommendation. In *Proceedings of the Eighteenth ACM International Conference on Web Search and Data Mining*, pages 300–308.
- JI Nelson and BJ Frost. 1978. Orientation-selective inhibition from beyond the classic visual receptive field. *Brain research*, 139(2):359–365.
- Marek Rei and Anders Søgaard. 2019. Jointly learning to label sentences and tokens. In *Proceedings of the AAAI Conference on Artificial Intelligence*, volume 33, pages 6916–6923.
- Michael P Sceniak, Dario L Ringach, Michael J Hawken, and Robert Shapley. 1999. Contrast’s effect on spatial summation by macaque v1 neurons. *Nature neuroscience*, 2(8):733–739.
- Joe Stacey, Yonatan Belinkov, and Marek Rei. 2022. Supervising model attention with human explanations for robust natural language inference. In *Proceedings of the AAAI conference on artificial intelligence*, volume 36, pages 11349–11357.
- Jianlin Su, Jiarun Cao, Weijie Liu, and Yangyiwen Ou. 2021. Whitening sentence representations for better semantics and faster retrieval. *arXiv preprint arXiv:2103.15316*.
- I Tenney. 2019. Bert rediscovers the classical nlp pipeline. *arXiv preprint arXiv:1905.05950*.
- Liang Wang, Nan Yang, Xiaolong Huang, Linjun Yang, Rangan Majumder, and Furu Wei. 2024. Improving text embeddings with large language models. *arXiv preprint arXiv:2401.00368*.
- Benjamin Warner, Antoine Chaffin, Benjamin Clavié, Orion Weller, Oskar Hallström, Said Taghadouini, Alexis Gallagher, Raja Biswas, Faisal Ladhak, Tom Aarsen, et al. 2024. Smarter, better, faster, longer: A modern bidirectional encoder for fast, memory efficient, and long context finetuning and inference. *arXiv preprint arXiv:2412.13663*.
- Sanghyun Woo, Jongchan Park, Joon-Young Lee, and In So Kweon. 2018. Cbam: Convolutional block attention module. In *Proceedings of the European Conference on Computer Vision (ECCV)*, pages 3–19.
- Kai Xu, Minghai Qin, Fei Sun, Yuhao Wang, Yen-Kuang Chen, and Fengbo Ren. 2020. Learning in the frequency domain. In *Proceedings of the IEEE/CVF conference on computer vision and pattern recognition*, pages 1740–1749.
- Jianxiang Zang and Hui Liu. 2023a. How to extract and interact? nested siamese text matching with interaction and extraction. In *International Conference on Artificial Neural Networks*, pages 523–535. Springer.
- Jianxiang Zang and Hui Liu. 2023b. Improving text semantic similarity modeling through a 3d siamese network. In *ECAI 2023*, pages 2970–2977. IOS Press.
- Jianxiang Zang and Hui Liu. 2024a. Explanation based bias decoupling regularization for natural language inference. In *2024 International Joint Conference on Neural Networks (IJCNN)*, pages 1–8. IEEE.
- Jianxiang Zang and Hui Liu. 2024b. Modeling selective feature attention for representation-based siamese text matching. *arXiv preprint arXiv:2404.16776*.
- Jianxiang Zang, Meiling Ning, Shihan Dou, Jiazheng Zhang, Tao Gui, Qi Zhang, and Xuanjing Huang. 2025a. Mitigating attention hacking in preference-based reward modeling via interaction distillation. *arXiv preprint arXiv:2508.02618*.
- Jianxiang Zang, Meiling Ning, Yongda Wei, Shihan Dou, Jiazheng Zhang, Nijia Mo, Binhong Li, Tao Gui, Qi Zhang, and Xuanjing Huang. 2025b. Compression hacking: A supplementary perspective on informatics metric of language models from geometric distortion. *arXiv preprint arXiv:2505.17793*.

Yan Zhang, Ruidan He, Zuozhu Liu, Kwan Hui Lim, and Lidong Bing. 2020. An unsupervised sentence embedding method by mutual information maximization. In *Proceedings of the 2020 Conference on Empirical Methods in Natural Language Processing (EMNLP)*, pages 1601–1610.

Yanzhao Zhang, Richong Zhang, Samuel Mensah, Xudong Liu, and Yongyi Mao. 2022. Unsupervised sentence representation via contrastive learning with mixing negatives. In *Proceedings of the AAAI Conference on Artificial Intelligence*, volume 36, pages 11730–11738.

Penghao Zhao, Hailin Zhang, Qinhan Yu, Zhengren Wang, Yunteng Geng, Fangcheng Fu, Ling Yang, Wentao Zhang, Jie Jiang, and Bin Cui. 2024. Retrieval-augmented generation for ai-generated content: A survey. *arXiv preprint arXiv:2402.19473*.

Zhi Zheng, Wenshuo Chao, Zhaopeng Qiu, Hengshu Zhu, and Hui Xiong. 2024. Harnessing large language models for text-rich sequential recommendation. In *Proceedings of the ACM Web Conference 2024*, pages 3207–3216.

Dawei Zhu, Liang Wang, Nan Yang, Yifan Song, Wenhao Wu, Furu Wei, and Sujian Li. 2024. Longembed: Extending embedding models for long context retrieval. In *Proceedings of the 2024 Conference on Empirical Methods in Natural Language Processing*, pages 802–816.

Yutao Zhu, Huaying Yuan, Shuting Wang, Jiongnan Liu, Wenhan Liu, Chenlong Deng, Haonan Chen, Zheng Liu, Zhicheng Dou, and Ji-Rong Wen. 2023. Large language models for information retrieval: A survey. *arXiv preprint arXiv:2308.07107*.

Wenjie Zhuo, Yifan Sun, Xiaohan Wang, Linchao Zhu, and Yi Yang. 2023. Whitenedcse: Whitening-based contrastive learning of sentence embeddings. In *Proceedings of the 61st Annual Meeting of the Association for Computational Linguistics (Volume 1: Long Papers)*, pages 12135–12148.

A Contrastive Learning

We applied contrastive learning for training sentence embeddings. The contrastive loss requires pairs of examples, $\mathcal{B} = \{(\mathbf{v}_d, \mathbf{v}_d^+)\}$, as a batch in the training set, where \mathbf{v}_d represents sentence representation *after pooling* and \mathbf{v}_d^+ represents a representation of a relevant positive example (one that is semantically similar). During unsupervised training, \mathbf{v}_d^+ serves as the positive example for \mathbf{v}_d , while all other samples in the batch are treated as negatives. The model is trained to bring positives closer and push negatives away. We employed batch-sampled softmax to construct our contrastive

loss, as formulated in Equation 12. Here, \mathcal{B} represents a training batch, and τ is the softmax temperature. We use cosine similarity as the similarity function $\mathcal{F}_{\text{sim}}(\mathbf{v}_d, \mathbf{v}_d^+) = \frac{\mathbf{v}_d^T \cdot \mathbf{v}_d^+}{\|\mathbf{v}_d\| \|\mathbf{v}_d^+\|}$.

$$\mathcal{L} = -\log \frac{\exp(\frac{\mathcal{F}_{\text{sim}}(\mathbf{v}_d, \mathbf{v}_d^+)}{\tau})}{\sum_{k \in \mathcal{B}} \exp(\frac{\mathcal{F}_{\text{sim}}(\mathbf{v}_d, \mathbf{v}_k^+)}{\tau})} \quad (12)$$

It is worth noting that when pooling 2D sentence representations into 1D representations, there are generally two options: using the [CLS] representation or the average of all token representations. In this section, we discuss the impact of these two pooling methods on sentence vectors when introducing S²Sent. Table 3 discusses the impact of different sentence embedding pooling on sentence vectors trained with SimCSE and reports the average of STS. We were surprised to find that without the introduction of S²Sent, there was no significant difference between the results of [CLS] and Avg.. However, when S²Sent was introduced, the performance of sentence embeddings using [CLS] pooling experienced a surprisingly sharp decline. This is because the [CLS] representation of different blocks captures the semantic information of each block, but unlike the Avg. pooling, the [CLS] representation does not have a linear relationship with the token representations when weighted and fused through S²Sent, losing most of its semantic information and its original meaning. Therefore, we strongly advocate for the use of average pooling to obtain the 1D embedding of sentences for downstream contrastive learning.

Pooling	BERT	+S ² Sent
CLS	76.21	66.88
Avg.	76.22	78.50
Pooling	RoBERTa	+S ² Sent
CLS	76.65	61.17
Avg.	76.46	78.48

Table 3: The impact of different sentence embedding pooling on the training of sentence embedding with SimCSE.

B Transfer Tasks

We also evaluated our model on the following transfer tasks: MR, CR, SUBJ, MPQA, SST-2, TREC, and MRPC. We followed the default configurations in SentEval. The results are shown in Table 4. It can

be observed that after the introduction of S2Sent, the baseline showed significant improvements on most of the benchmarks.

C SS Motivation’s Supplementary Explanation

We explained in the main text that after SS introduced multi-scale adaptive fusion, the coefficient in front of each $\prod_{k=0}^n \frac{\partial \mathbf{u}^{(k)}}{\partial \mathbf{u}^{(k-1)}}$ is $\mathcal{K} = \mathbf{e}^{(n)} + \frac{\partial \mathbf{v}}{\partial \mathbf{U}}$, which is related to n . Under the condition of directly linearly fusing different Transformer blocks traditionally, \mathcal{K} is either a constant or a gradient value unrelated to n . We will analyze gradient management under linear fusion in this part, that is, the case of not assigning adaptive weights to each block. The aggregation of each Transformer’s representation \mathbf{U} is multiplied element-wise with its feature embedding, resulting in $\mathbf{v} = \mathbf{e} * \mathbf{U}$. The gradient flow chain is jointly determined by the two gradient propagations of \mathbf{e} and \mathbf{U} , that is, $\frac{\partial \mathbf{v}}{\partial \mathbf{U}} = \mathbf{e}$ and $\frac{\partial \mathbf{v}}{\partial \mathbf{e}} = \mathbf{U}$. The gradient flow in the direction of \mathbf{e} is shown in Equation 13.

$$\frac{\partial \mathbf{v}}{\partial \mathbf{U}}|_{w/o} = \frac{\partial \mathbf{v}}{\partial \mathbf{e}} * \frac{\partial \mathbf{e}}{\partial \mathbf{s}} * \frac{\partial \mathbf{s}}{\partial \mathbf{v}} * \frac{\partial \mathbf{v}}{\partial \mathbf{U}} \quad (13)$$

Combining the gradient backpropagation of $\mathbf{u}^{(n)} \rightarrow \mathbf{U}$, the calculation of the total gradient flow is shown in Equation 14. Where $\mathbf{u}^{(n)} \rightarrow \mathbf{U}$ is a stacked linear connection, hence $\frac{\partial \mathbf{x}}{\partial \mathbf{x}^{(n)}}$ is a constant. To simplify notation, we take it as 1 and omit it in the Equation 14.

$$\begin{aligned} \frac{\partial \mathbf{v}}{\partial \mathbf{u}^{init}}|_{w/o} &= 2 * \frac{\partial \mathbf{v}}{\partial \mathbf{U}} * \sum_{n=0}^{N-1} \frac{\partial \mathbf{U}}{\partial \mathbf{u}^{(n)}} * \prod_{k=0}^n \frac{\partial \mathbf{u}^{(k)}}{\partial \mathbf{u}^{(k-1)}} \\ &= 2 * \frac{\partial \mathbf{v}}{\partial \mathbf{U}} * \sum_{n=0}^{N-1} \prod_{k=0}^n \frac{\partial \mathbf{u}^{(k)}}{\partial \mathbf{u}^{(k-1)}} \end{aligned} \quad (14)$$

It can be observed that the gradient flow for feature extraction in each Transformer block, $\prod_{k=0}^n \frac{\partial \mathbf{u}^{(k)}}{\partial \mathbf{u}^{(k-1)}}$, affects the total gradient flow in the same proportion as $2 * \frac{\partial \mathbf{v}}{\partial \mathbf{U}}$. This indicates that the parameters of each Transformer block are updated to the same extent. However, this does not meet the requirement for differentiated gradient flow management of semantic features at different scales, resulting in the feature extraction capabilities of different blocks within the Transformer not being fully unleashed.

Method	MR	CR	SUBJ	MPQA	SST-2	TREC	MRPC	Avg.
SimCSE-BERT	81.01	86.19	94.45	89.28	85.10	89.40	74.51	85.71
+S ² Sent	80.95	86.79	95.12	89.97	86.12	89.97	74.98	86.27
PromptBERT	80.69	85.89	93.81	89.87	84.89	88.48	76.28	85.70
+S ² Sent	81.45	86.64	93.91	89.91	84.77	89.52	76.99	86.17
SimCSE-RoBERTa	81.15	87.14	93.29	86.14	86.50	84.43	73.28	84.56
+S ² Sent	82.01	87.89	93.96	85.91	86.94	85.23	74.02	85.14
Prompt-RoBERTa	83.72	88.59	93.37	90.40	88.10	90.01	76.27	87.21
+S ² Sent	83.44	88.90	93.01	90.77	88.64	90.08	76.43	87.32

Table 4: Transfer task results of different sentence embedding models. The bolded values represent results that show significant improvement relative to the baseline (t-test).